

Magnetic spin moment reduction in photoexcited ferromagnets through exchange interaction quenching: Beyond the rigid band approximation

G. P. Zhang^{1,*}, M. S. Si², Y. H. Bai³, and Thomas F. George⁴

¹*Department of Physics, Indiana State University, Terre Haute, IN 47809, USA*

²*Key Laboratory for Magnetism and Magnetic Materials of the Ministry of Education, Lanzhou University, Lanzhou 730000, China*

³*Office of Information Technology, Indiana State University, Terre Haute, IN 47809, USA and*

⁴*Office of the Chancellor and Center for Nanoscience Departments of Chemistry & Biochemistry and Physics & Astronomy University of Missouri-St. Louis, St. Louis, MO 63121, USA*

(Dated: October 14, 2018)

Abstract

The exchange interaction among electrons is one of the most fundamental quantum mechanical interactions in nature and underlies any magnetic phenomena from ferromagnetic ordering to magnetic storage. The current technology is built upon a thermal or magnetic field, but a frontier is emerging to directly control magnetism using ultrashort laser pulses. However, little is known about the fate of the exchange interaction. Here we report unambiguously that photoexcitation is capable of quenching the exchange interaction in all three *3d* ferromagnetic metals. The entire process starts with a small number of photoexcited electrons which build up a new and self-destructive potential that collapses the system into a new state with a reduced exchange splitting. The spin moment reduction follows a Bloch-like law as $M_z(\Delta E) = M_z(0)(1 - \Delta E/\Delta E_0)^{\frac{1}{\beta}}$, where ΔE is the absorbed photon energy and β is a scaling exponent. A good agreement is found between the experimental and our theoretical results. Our findings may have a broader implication for dynamic electron correlation effects in laser-excited iron-based superconductors, iron borate, rare-earth orthoferrites, hematites and rare-earth transition metal alloys.

PACS numbers: 75.78.Jp, 75.40.Gb, 78.20.Ls, 75.70.-i

1. INTRODUCTION

Ultrafast laser technology fuels unprecedented investigations in physics, chemistry, material science and technology. Using a femtosecond laser pulse to steer chemical reactions is the foundation of femtochemistry (Nobel prize in chemistry in 1999) [1]. This inspires the development of femtosecond Raman [2] and 2D IR spectroscopy [3]. A strong and ultrafast laser pulse can rip off and drive back electrons from gaseous atoms to generate high order harmonic generations, with emitted energy exceeding 200 eV and with time duration on the order of several hundred attoseconds ($1 \text{ as} = 10^{-18} \text{ s}$), representing an era of attophysics [4]. Ultrafast dynamics and fragmentation of C_{60} were investigated under intense laser pulses [5]. Ultrafast laser pulses can coherently control the four-wave mixing signals in GaAs [6]. Efforts in superconductors started one decade ago, with an enormous success, for some latest discoveries, see [7–10]. A strong laser field can even induce a transient superconductivity above T_c in $YBa_2Cu_3O_{7-\delta}$ [11], and reveals the competition between the pseudogap and superconducting states [12]. An ultrafast laser allows one to investigate charge, spin and lattice dynamics in complex materials. Just within a week, a flurry of three research papers [13–15] reported photoinduced dynamics in three entirely different systems: lattice dynamics in high-temperature iron pnictide superconductors [13], exchange parameter modification in iron oxides [15], and orbital magnetism in multisublattice metallic magnets [14].

Laser-induced ultrafast demagnetization represents a major breakthrough in magnetism. Beaurepaire and his colleagues [16] demonstrated that a femtosecond laser pulse can induce an ultrashort demagnetization in fcc Ni within 1 ps. This field, which is termed femtomagnetism, is rapidly growing [17, 18], with nonthermal switching observed [19, 20], and motivated new developments in table-top high harmonic probe in complex magnetic materials at M-edge, which is normally only accessible using synchrotron radiation [21]. Coherent ultrafast magnetism is also discovered by Barthelemy and colleagues [22, 23]. A new comprehensive review is presented at the first conference on ultrafast magnetism [24].

Despite the enormous progress experimentally, theoretical understanding falls behind. In superconductors, besides an early attempt [25], only one study [15] presented a theoretical analysis, but it does not catch the initial excitation of electrons and subsequent change in the spin exchange interaction [26]. In magnetic materials, Sandratskii and Mavropoulos [27] found that the Elliott-Yafet mechanism [28] plays an important role in femtomagnetic

properties of FeRh, which complements the superdiffusive mechanism [29] and the laser-spin-orbit coupling mechanism [30, 31]. One important feature of these prior theoretical studies is that they do not allow band structures to change. This rigid band approximation has already been proven inadequate for simple $3d$ transition metals [32–36].

For instance, our first-principles calculation shows that under the rigid band approximation the induced spin change is less than 1% [37–39]. There are several reasons why the spin change is small. Si *et al.* [40] showed that due to the laser photon energy $\hbar\omega$, only those transitions whose transition energy ΔE matches $\hbar\omega$ can be strongly excited, while others are optically silent. This limits on the number of electrons that can be excited. Once the number of excited electrons is small, then the spin change is likely to be small. Essert and Schneider [32] further showed that even including the electron-phonon interaction and the electron-electron interaction [33], the spin moment change is very small. In 2013, Mueller and coworkers [35] employed a simple model system but included a feedback from the charge change; they found a substantial spin reduction. Krieger *et al.* [36] carried out the time-dependent density functional investigation and found that the spin reduction is comparable to the experimental one, although their laser fluences were about 2-3 orders of magnitude higher than experimental fluences.

Besides those initial theoretical efforts, no study on the exchange interaction change during photoexcitation has been carried out. Nevertheless, these studies point out a possible solution. It is possible that the band structure relaxation and self-consistency are essential to our current understanding of the demagnetization process in ferromagnets. The importance of research along this direction should not be under-estimated since it may have a broader implication in magnetic excitations in high-temperature superconductors. Ultrafast laser and x-ray technology has a unique capability to separate the spin excitation and phonon excitation on different time scales, and provides new insights into the nature of these elementary excitations. For instance, Chuang *et al.* [41] employed the time-resolved resonant x-ray diffraction to follow the strongly coupled spin and charge order parameters in stripe-ordered nickelate crystals. Smallwood *et al.* [42] showed that one can even track the Cooper pairs dynamics by ultrafast angle-resolved photoemission. These experimental findings are exciting. A theoretical investigation on the exchange interaction change during the photoexcitation is much needed.

Here we report the first density functional study of the exchange interaction quenching

during laser excitation. We first construct an excited potential energy surface by promoting a small number of electrons from the valence band to the conduction band. Even though the number of electrons actually excited is small, the excited-state potential is quite different from the ground-state potential when the excited state is a few eV above the Fermi level. Then we self-consistently solve the Kohn-Sham equation under this excited potential. This self-consistency triggers an avalanche on the entire system and importantly affects those unexcited electrons that are initially unexcited, so that the exchange splitting is sharply reduced. For all the three $3d$ ferromagnets, we observe a big reduction of spin moment. If we assume 12.5% absorption efficiency of photon energy into fcc Ni, we can reproduce the same amount of change observed experimentally [16]. Our theory can reproduce the entire range of experimental fluence-dependence of the spin moment change in bcc Fe [43] quantitatively for the same absorption efficiency. This is very encouraging. The key to our success is that we allow the full relaxation of the electronic band structure under the excited potential. We expect that our formalism will move us one step closer to reveal the true mechanism of femtomagnetism, and this may also present a reliable method to investigate the spin excitation in high temperature iron-based superconductors and metallic magnets for the spin switching.

This paper is arranged as follows. In Section 2, we present our ideas and theoretical scheme. Section 3 is devoted to the results and discussion on the demagnetization, band relaxation and exchange splitting reduction. We conclude our paper in Section 4.

2. THEORETICAL FORMALISM

Calculating excited states is traditionally a hard problem. The progress in this field is slow and very limited, in comparison with the ground state calculation. There is no easy and simple solution in sight. The enormous development in ultrafast laser technology presents new opportunities to investigate the charge and spin dynamics on the femtosecond time scale in multiple fronts from traditional high temperature superconductors, graphene, magnetic materials and layer structures, topological insulators and nanostructures, to name a few. Our effort represents a theoretical effort in this direction.

Figure 1 schematically summarizes our main idea. When a laser pulse impinges a magnet, it first promotes a few electrons from the valence band $|\mathbf{k}v\rangle$ to the conduction band $|\mathbf{k}c\rangle$

(see the bottom figure). Due to energy conservation, the energy change $\Delta E = E_{\mathbf{k}c} - E_{\mathbf{k}v}$ must be equal to the photon energy $\hbar\omega$ of the laser within an energy window δ (inversely proportional to the laser pulse duration). This initial excitation can already induce some spin change [30, 31, 38]; and more importantly, it directly affects the exchange interaction through

$$J(ab||ab) = \int \int d\mathbf{r}_1 d\mathbf{r}_2 \phi_a^*(\mathbf{r}_1) \phi_b^*(\mathbf{r}_2) \phi_a^*(\mathbf{r}_2) \phi_b^*(\mathbf{r}_1) |\mathbf{r}_1 - \mathbf{r}_2|^{-1}, \quad (1)$$

where $\phi_{a(b)}(\mathbf{r})$ is the wavefunction, and the integration is over the electron coordinate \mathbf{r} . For a free electron gas, with an increase in the kinetic energy, the exchange energy decreases as [44]

$$E_{ex}(k) = -\frac{2e^2}{\pi} k_f \left[\frac{1}{2} + \frac{1-x^2}{4x} \ln \left(\frac{1+x}{1-x} \right) \right], \quad (2)$$

where $x = k/k_f$ and k_f is the Fermi wavevector, and k is the electron wavevector.

In the density functional theory, the exchange energy $E_{ex}[\rho]$ is a functional of the electron density $\rho(\mathbf{r})$. The effect of the laser field enters through the excited density $\rho^{ex}(\mathbf{r}) = \sum_{\mathbf{k}n}^{occ} n_{\mathbf{k}n} = \sum_{\mathbf{k}n}^{occ} |\psi_{\mathbf{k}n}(\mathbf{r})|^2$, which self-consistently generates a new potential. $\psi_{\mathbf{k}n}$ is the Kohn-Sham wavefunction computed from [45]

$$\left[-\frac{\hbar^2}{2m} \nabla^2 + v_{ext}(\mathbf{r}) + e^2 \int \frac{\rho(\mathbf{r}')}{|\mathbf{r} - \mathbf{r}'|} d\mathbf{r}' + v_{xc}[\rho(\mathbf{r})] \right] \psi_{\mathbf{k}n}(\mathbf{r}) = E_{\mathbf{k}n} \psi_{\mathbf{k}n}(\mathbf{r}), \quad (3)$$

where the terms on the left-hand side are the kinetic energy, external potential, Coulomb and exchange-correlation potential energies, respectively. The spin-orbit coupling is included through the second variational principle [46]. $E_{\mathbf{k}n}$ and $\psi_{\mathbf{k}n}(\mathbf{r})$ are the eigenvalue and eigenwavefunction of state $\mathbf{k}n$.

The top portion of Fig. 1 shows the flow of our theoretical formalism. For a pair excitation from $|\mathbf{k}v\rangle$ to $|\mathbf{k}c\rangle$, we construct the excited charge density via [40]

$$\left. \begin{aligned} n_{\mathbf{k}c}^{ex}(\mathbf{r}) &= \alpha n_{\mathbf{k}v}(\mathbf{r}) + (1 - \alpha) n_{\mathbf{k}c}(\mathbf{r}) \\ n_{\mathbf{k}v}^{ex}(\mathbf{r}) &= \alpha n_{\mathbf{k}c}(\mathbf{r}) + (1 - \alpha) n_{\mathbf{k}v}(\mathbf{r}) \end{aligned} \right\} \quad \text{if } |E_{\mathbf{k}c} - E_{\mathbf{k}v} - \hbar\omega| \leq \delta, \quad (4)$$

where $n_{\mathbf{k}v}(\mathbf{r})$ and $n_{\mathbf{k}c}(\mathbf{r})$ are the charge densities for the valence band $\mathbf{k}v$ and conduction band $\mathbf{k}c$, respectively. The weighted occupation of the excitation, α , represents the strength of the excitation and changes from 0 to 1. If $\alpha = 0$, this is just a ground-state calculation; if the laser excitation is strong, α should be increased. If the excitation energy falls outside δ , no change is made to their occupation. For this reason, δ should be kept reasonably low,

less than 1 eV; if it is too wide, characters of valence and conduction bands may be quite different and vary a lot. This is particularly important for binary or ternary compounds.

Equation (4) is missing in all the previous rigid-band calculations. If the photoexcited valence and conduction bands had the same orbital character, whether Eq. (4) is included would not make a big difference. But for the laser excitation with a few eV above the Fermi level, the orbital characters of the valence and conduction bands are quite different. For this reason, we expect a huge effect on the entire system. Our method is similar to the excitation energy calculation in transition metal atoms by Vukajlovic [47] and rare-earth metals done by Herbst *et al.* [48], and more recently a photocarrier doping treatment [49] (and also quantum chemistry calculations). We implement our method using the Wien2k code, which uses the full-potential augmented planewave method. This code is among the most accurate density functional codes, and is cheaper than other commercial codes, with open source codes and well designed structures and directories (the reader is encouraged to contact us for the further implementation details). One of the biggest advantages over the pseudopotential codes is that it can be extended to the core level excitation which has been a hot topic for the experimental community. In our supplementary materials, we provide all the details about our implementation. Here, in brief, we summarize our major changes to the code. The first major change is made to the `lapw2`, where the new charge density and potential are constructed through the above equation 4. The second change is to add one input file which includes the laser photon energy and energy window. We revise the major scripts to run the code and also add four new files which store the number of electron excited and the pair indices of each excitation and their original weights.

3. RESULTS AND DISCUSSION

3.1 Demagnetization versus absorbed photon energy in Ni, Co and Fe

Since the beginning of femtomagnetism, a central question is how the spin moment reduction is correlated with the energy absorbed into a system. Figure 2(a) shows the spin moment in fcc Ni as a function of the absorbed energy ΔE by changing α , with the excitation window fixed at $\delta = 0.5$ eV. Here ΔE is defined as the total energy difference between the before-and-after electron excitation, which is also called the promotion energy [47]. As

the promotion energy increases, we find the spin moment drops sharply. This dependence can be fitted to a scaling that resembles the magnetization curve,

$$M_z(\Delta E) = M_z(0)\left(1 - \frac{\Delta E}{\Delta E_0}\right)^{\frac{1}{\beta}}, \quad (5)$$

where for fcc Ni, we find $M_z(0) = 0.63\mu_B$, $\Delta E_0 = 1.48$ eV, and $\beta = 2.6$. With this curve, in principle, we can compute the average spin moment up to the penetration depth d as

$$\bar{M}_z = \sum_{l=0}^L M_z(\Delta E_l)/L, \quad (6)$$

where L is the number of atomic layers up to the penetration depth, and l is the layer index. Unfortunately, the energy absorbed at each layer is unknown and depends on the thickness of the sample, as shown by Schellekens *et al.* [50], but no expression is given. We assume that the absorbed energy is proportional to the light energy times an absorption efficiency factor η , or $\Delta E_l = \frac{1}{2}\eta E_{light} \exp(-la/2d)$, where E_{light} is the light energy at the top of the sample [40] and a is the lattice constant. For any energy higher than ΔE_0 , the spin moment is zero. At the penetration depth, $\Delta E_l = \frac{1}{2}\eta E_{light}/e$. The red line in Fig. 2(a) denotes the experimental reduction (50%) [16]. We find that to have the same experimental spin moment reduction at the penetration depth, $\eta = 12.5\%$ is enough. Obviously this η is the most conservative estimate and represents an uplimit since layers above the penetration depth must have stronger demagnetization and by average the spin reduction is larger than the experimental value. This η presents an opportunity for the experimentalist to verify our theoretical prediction.

We apply our theory to hcp Co (Fig. 2(b)) and bcc Fe (Fig. 2(c)). We see a similar spin reduction for hcp Co. Once the absorbed energy is above 1.7 eV, the spin moment is quenched completely. This critical energy is higher than in fcc Ni, since hcp Co has a higher Curie temperature and is harder to be demagnetized. The most difficult case is bcc Fe. To reduce its spin moment by 50%, one needs one photon per atom, which is consistent with the experimental results. Mathias *et al.* [51] found that in the same experiment the Ni spin moment is quenched by 45%, while the Fe spin moment is quenched by only 19%.

Up to now, all the comparisons between the experiments and our theoretical results focus on a single laser fluence. Weber *et al.* [43] systematically investigated the dependence of spin moment reduction in Fe on the pump pulse fluence. This presents an excellent test case for our theory over a range of five pump fluences; and we only have one tuning parameter η .

It is important to point out that tuning η changes either the slope of the spin moment versus the absorbed energy [$M_z - \Delta E$ curve in Fig. (2)] or the absolute energy, but not both. We use the same method as above and find that only $\eta = 12.5\%$ allows us to match both the absolute energy absorbed and the slope of $M_z - \Delta E$ curve. Figure 2(c) shows that their experimental results (empty filled boxes) agree our theoretical data (empty circles) within a few percentage. Such a quantitative agreement is encouraging as it gives us more confidence in our first-principles methods. From the comparison between bcc Fe and fcc Ni, we see that η shows a weak dependence on the material in question, but this may be due to the similarity between bcc Fe and fcc Ni. Additional testing and investigation is necessary using other materials [52, 53]. To compare the theoretical and experimental results, we need the energy absorbed for each layer, ideally starting from one monolayer, grown on a transparent substrate so little photon energy is absorbed into the substrate. To minimize the heating effect, we suggest to use a shorter laser pulse and lower repetition rate. This also suppresses the phonon contribution, and targets on the magnetic excitation alone.

3.2 Band relaxation and exchange splitting reduction

The exchange splitting reduction and transient band structures are clearly observed experimentally in gadolinium and terbium [54]. Teichmann and colleagues [55] found that in Gd, the spin-down band moves down by 0.07 eV and the spin-up band moves up by 0.2 eV; in Tb, the shifts are 0.16 eV for both spin channels. These experimental results are consistent with an earlier study in fcc Ni [56].

To reveal some crucial insights into the demagnetization, we employ fcc Ni as an example and start with our ground-state calculation, whose density of d -states (DOS) is shown in Fig. 3(a), where the Fermi energy is at zero. The exchange splitting between the majority and minority spin DOS maxima is 0.82 eV. Figure 3(b) shows the DOS for the excited-state configuration, where $\alpha = 0.7$ and $\delta = 0.5$ eV. While the excited DOS shape does not change much, the majority and minority bands are clearly shifted, with the larger shift in the majority band by as much as 0.5 eV toward the Fermi level. The splitting is reduced to 0.24 eV, consistent with the experimental findings [56]. The exchange splitting reduction is a precursor to the spin moment decrease.

3.3 Spin moment reduction as the excited potential surface relaxes

We can reveal further details how the spin moment is reduced during the self-consistent iterations. As an example, we use the same α and δ as Fig. 2. The laser photon energy is also fixed at $\hbar\omega = 2.0$ eV. Figure 3(c) shows that for the first two iterations the spin moment change is very small, by about $0.02 \mu_B$, or about 3%. However, this is already far larger than the spin moment change found in our rigid-band simulation [37, 57]. This further confirms our earlier observation [40] that even though the electrons are promoted to the excited states, the spin moment change is very small in all the rigid band calculations. The main reason is because the number of electrons excited is only limited to those \mathbf{k} points where the transition energies match the photon energy. Electrons at other \mathbf{k} points have no contribution to the spin moment change. After the third iteration, the excited potential generated by those excited electrons has a dramatic impact on the entire system; as a result, the spin moment drops precipitously. Figure 2(d) shows that the spin gradually converges to $0.23 \mu_B$, with a net reduction of $0.4 \mu_B$, or 63%. This high percentage spin loss is consistent with the experimental findings.

3.4 Effects of the excitation strength and excitation window

To have a clear view as to how the level of excitation affects the spin moment change, we keep the excitation energy window fixed and gradually increase α . The empty circles in Fig. 3(e) show that as α increases from 0 to 0.8, the spin moment is reduced precipitously and completely quenched at $\alpha = 0.8$. We also calculate the number of electrons actually excited. The filled boxes in Fig. 3(e) show how the number of excited electrons changes with α . In all the cases, the number of electrons excited is below 1. Quantitatively, we find that at $\alpha = 0.1$, the number of electrons excited is 0.13, and the spin reduction is $0.03 \mu_B$, or $0.23 \mu_B$ per electron. At $\alpha = 0.7$, ‘0.7 electron’ is excited out of 10 valence electrons, and the spin is reduced by $0.4 \mu_B$, so that for each electron excited, the spin is reduced by $0.57 \mu_B$. This unambiguously demonstrates the importance of the self-consistency and the band relaxation.

The excitation weight is not the only parameter that affects the spin – so does the excitation energy window δ . Energetically, a larger window corresponds to a shorter laser

pulse. With a larger δ , more states enter the excitation window. Figure 3(f) shows that as the window becomes wider, a sharper reduction is observed, but the change is not completely monotonic, since the states moving in and out of the excitation window are not continuous (see the density of states in Fig. 3(a)). We should emphasize again that the value of δ should be relatively small, less than 1 eV. In some cases, this also affects the convergence (see the supplementary materials for details) [45].

4. CONCLUSIONS

Through the first-principles density functional theory, we have demonstrated unambiguously that even a small number of electrons excited can lead to a strong quenching in the exchange interaction. This process occurs through a band relaxation across the entire Brillouin zone. The electrons in the excited states build a self-destructive potential that greatly weakens the electron correlation effect and reduces the exchange splitting. As a direct consequence, the strong demagnetization is induced and the exchange splitting is reduced, consistent with the experimental results [56]. This resolves one of the most difficult puzzles in femtomagnetism. Our finding has a broader implication on the ultrafast dynamics in iron pnictides since the laser can even change the lattice structures [13] and the exchange interaction must be changed as well. In iron oxides, the effect is even more important [15]. For the first time, our study establishes a different paradigm: During the laser excitation it is the excitation of electrons that impacts on the exchange interaction and spin moment, while the effect of the spin fluctuation on the exchange interaction is secondary and is on a much longer time scale.

This work was solely supported by the U.S. Department of Energy under Contract No. DE-FG02-06ER46304. Part of the work was done on Indiana State University’s quantum cluster and high-performance computers. The research used resources of the National Energy Research Scientific Computing Center, which is supported by the Office of Science of the U.S. Department of Energy under Contract No. DE-AC02-05CH11231. This work was performed, in part, at the Center for Integrated Nanotechnologies, an Office of Science User Facility operated for the U.S. Department of Energy (DOE) Office of Science by Los Alamos National Laboratory (Contract DE-AC52-06NA25396) and Sandia National Laboratories (Contract DE-AC04-94AL85000).

- [1] A. H. Zewail, *Pure Appl. Chem.* **72**, 2219 (2000).
- [2] W. Wang *et al.*, *PNAS* **110**, 18397 (2013).
- [3] M. J. Tucker *et al.*, *PNAS* **110**, 17314 (2013).
- [4] P. H. Bucksbaum, *Nature* **421**, 593 (2002).
- [5] Z. Z. Lin and X. Chen, *Physics Letters A* **377**, 797 (2013)
- [6] Q. T. Vu *et al.*, *Phys. Rev. Lett.* **89**, 3508 (2000).
- [7] R. A. Kaindl *et al.*, *Science* **287**, 470 (2000).
- [8] R. D. Averitt *et al.*, *Phys. Rev. B* **63**, 140502 (2001).
- [9] N. Gedik *et al.*, *Phys. Rev. Lett.* **95**, 117005 (2005).
- [10] J. Demsar *et al.*, *Phys. Rev. Lett.* **82**, 4918, (1999).
- [11] S. Kaiser *et al.*, arxiv: 1205.4661 (2012).
- [12] G. Coslovich *et al.*, *Phys. Rev. Lett.* **110**, 107003 (2013).
- [13] S. Gerber, K. W. Kim, Y. Zhang, D. Zhu, N. Plonka, M. Yi, G. L. Dakovski, D. Leuenberger, P. S. Kirchmann, R. G. Moore, M. Chollet, J. M. Glowina, Y. Feng, J.-S. Lee, A. Mehta, A. F. Kemper, T. Wolf, Y.-D. Chuang, Z. Hussain, C.-C. Kao, B. Moritz, Z.-X. Shen, T. P. Devereaux, and W.-S. Lee, arXiv:1412.6842 (2014).
- [14] T. J. Huisman, R. V. Mikhaylovskiy, A. Tsukamoto, Th. Rasing, and A. V. Kimel, arXiv:1412.5396 (2014).
- [15] R. V. Mikhaylovskiy, E. Hendry, A. Secchi, J. H. Mentink, M. Eckstein, A. Wu, R. V. Pisarev, V. V. Kruglyak, M. I. Katsnelson, Th. Rasing, and A. V. Kimel, arXiv:1412.7094 (2014).
- [16] E. Beaurepaire, J. -C. Merle, A. Daunois, and J.-Y. Bigot, *Phys. Rev. Lett.* **76**, 4250 (1996).
- [17] G. P. Zhang, W. Hübner, E. Beaurepaire, and J.-Y. Bigot, *Topics Appl. Phys.* **83**, 245 (2002).
- [18] A. Kirilyuk, A. V. Kimel, and Th. Rasing, *Rev. Mod. Phys.* **82**, 2731 (2010).
- [19] C. D. Stanciu, F. Hansteen, A. V. Kimel, A. Kirilyuk, A. Tsukamoto, A. Itoh, and Th. Rasing, *Phys. Rev. Lett.* **99**, 047601 (2007).
- [20] S. Mangin *et al.*, *Nature Materials* **13**, 286 (2014).
- [21] C. Stamm, T. Kachel, N. Pontius, R. Mitzner, T. Quast, K. Holldack, S. Khan, C. Lupulescu, E.F. Aziz, M. Wietstruk, H. A. Dürr, W. Eberhardt, *Nat. Mater.* **6**, 740 (2007).

- [22] M. Barthelemy, M. Sanches Piaia, M. Vomir, H. Vonesh, J.-Y. Bigot, *Ultrafast Magnetism I*, edited by J.-Y. Bigot *et al.*, Springer Proceedings in Physics **159**, page 214 (2015).
- [23] J.-Y. Bigot, M. Vomir, and E. Beaurepaire, *Nature Phys.* **5**, 515 (2009).
- [24] J.Y. Bigot, W. Hübner, Th. Rasing, and R. Chantrell, *Ultrafastmagnetism I*, Springer Proceedings in Physics, Vol. 159 (2015)
- [25] M. Sentef *et al.*, *Phys. Rev. X* **3**, 041033 (2013).
- [26] G. P. Zhang, M. Q. Gu and X. S. Wu, *J. Phys.: Condens. Matter* **26**, 376001 (2014).
- [27] L. M. Sandratskii and P. Mavropoulos, *Phys. Rev. B* **83**, 174408 (2011).
- [28] B. Koopmans *et al.*, *Nat. Mater.* **9**, 259 (2010).
- [29] M. Battiato, K. Carva, and P. M. Oppeneer, *Phys. Rev. Lett.* **105**, 027203 (2010).
- [30] G. P. Zhang and W. Hübner, *Phys. Rev. Lett.* **85**, 3025 (2000).
- [31] G. P. Zhang, W. Hübner, G. Lefkidis, Y. Bai, and T. F. George, *Nat. Phys.* **5**, 499 (2009).
- [32] S. Essert and H. C. Schneider, *Phys. Rev. B* **84**, 224405 (2011).
- [33] M. Krauß, T. Roth, S. Alebrand, D. Steil, M. Cinchetti, M. Aeschlimann, and H. C. Schneider, *Phys. Rev. B* **80**, 180407(R) (2009).
- [34] A. J. Schellekens and B. Koopmans, *Phys. Rev. Lett.* **110**, 217204 (2013).
- [35] B. Y. Mueller, A. Baral, S. Vollmar, M. Cinchetti, M. Aeschlimann, H. C. Schneider, and B. Rethfeld, *Phys. Rev. Lett.* **111**, 167204 (2013).
- [36] K. Krieger, J. K. Dewhurst, P. Elliott, S. Sharma, and E. K. U. Gross, arXiv: 1406.6607 (2014).
- [37] G. P. Zhang, Y. Bai, W. Hübner, G. Lefkidis, and T. F. George, *J. Appl. Phys.* **103**, 07B113 (2008).
- [38] G. P. Zhang, Y. Bai, and T. F. George, *Phys. Rev. B* **80**, 214415 (2009).
- [39] G. P. Zhang, M. S. Si, and T. F. George, *Journal of Applied Physics* **117**, 17D706 (2015).
- [40] M. S. Si and G. P. Zhang, *AIP Advances* **2**, 012158 (2012).
- [41] Y. D. Chuang, W. S. Lee, Y. F. Kung, A. P. Sorini, B. Moritz, R. G. Moore, L. Patthey, M. Trigo, D.-H. Lu, P. S. Kirchmann, M. Yi, O. Krupin, M. Langner, Y. Zhu, S. Y. Zhou, D. A. Reis, N. Huse, J. S. Robinson, R. A. Kaindl, R. W. Schoenlein, S. L. Johnson, M. Forst, D. Doering, P. Denes, W. F. Schlotter, J. J. Turner, T. Sasagawa, Z. Hussain, Z.-X. Shen, T. P. Devereaux, *Phys. Rev. Lett.* **110**, 127404 (2013).
- [42] C. L. Smallwood *et al.*, *Science* **336**, 1137 (2012).

- [43] A. Weber, F. Pressacco, S. Günther, E. Mancini, P. M. Oppeneer, and C. H. Back, *Phys. Rev. B* **84**, 132412 (2011).
- [44] N. W. Ashcroft and N. D. Mermin, *Solid State Physics* (Harcourt, 1976).
- [45] See the supplementary materials for the implementation details and the underlying rationale for our scheme.
- [46] P. Blaha, K. Schwarz, G. K. H. Madsen, D. Kvasnicka, and J. Luitz. WIEN2k: An augmented plane wave + local orbitals program for calculating crystal properties (Karlheinz Schwarz, Techn. Universität Wien, Austria, 2001).
- [47] F. R. Vukajlovic, E. L. Shirley, and R. M. Martin, *Phys. Rev. B* **43**, 3994 (1991).
- [48] J. F. Herbst, R. E. Watson, and J. W. Wilkins. *Phys. Rev. B* **17**, 3089 (1978).
- [49] D. Wegkamp, M. Herzog, L. Xian, M. Gatti, P. Cudazzo, C. L. McGahan, R. E. Marvel, R. F. Haglund, A. Rubio, M. Wolf *et al.*, arXiv: 1408.3209 (2014).
- [50] A. J. Schellekens, W. Verhoeven, T. N. Vader, and B. Koopmans, *Appl. Phys. Lett.* **102**, 252408 (2013).
- [51] S. Mathias *et al.*, *PNAS* **109**, 4792 (2012).
- [52] E. Beaupaire, M. Maret, V. Halte, J.-C. Merle, A. Daunois, and J.-Y. Bigot, *Phys. Rev. B* **58**, 12134 (1998).
- [53] C. Boeglin, E. Beaupaire, V. Halte, V. Lopez-Flores, C. Stamm, N. Pontius, H. A. Dürr, and J.-Y. Bigot, *Nature* **465**, 458 (2010).
- [54] R. Carley *et al.*, *Phys. Rev. Lett.* **109**, 057401 (2012).
- [55] M. Teichmann *et al.*, *Phys. Rev. B* **91**, 014425 (2015).
- [56] H. S. Rhie, H. A. Dürr, and W. Eberhardt, *Phys. Rev. Lett.* **90**, 247201 (2003).
- [57] T. Hartenstein, G. Lefkidis, W. Hübner, G. P. Zhang, and Yihua Bai, *J. Appl. Phys.* **105**, 07D305 (2009).

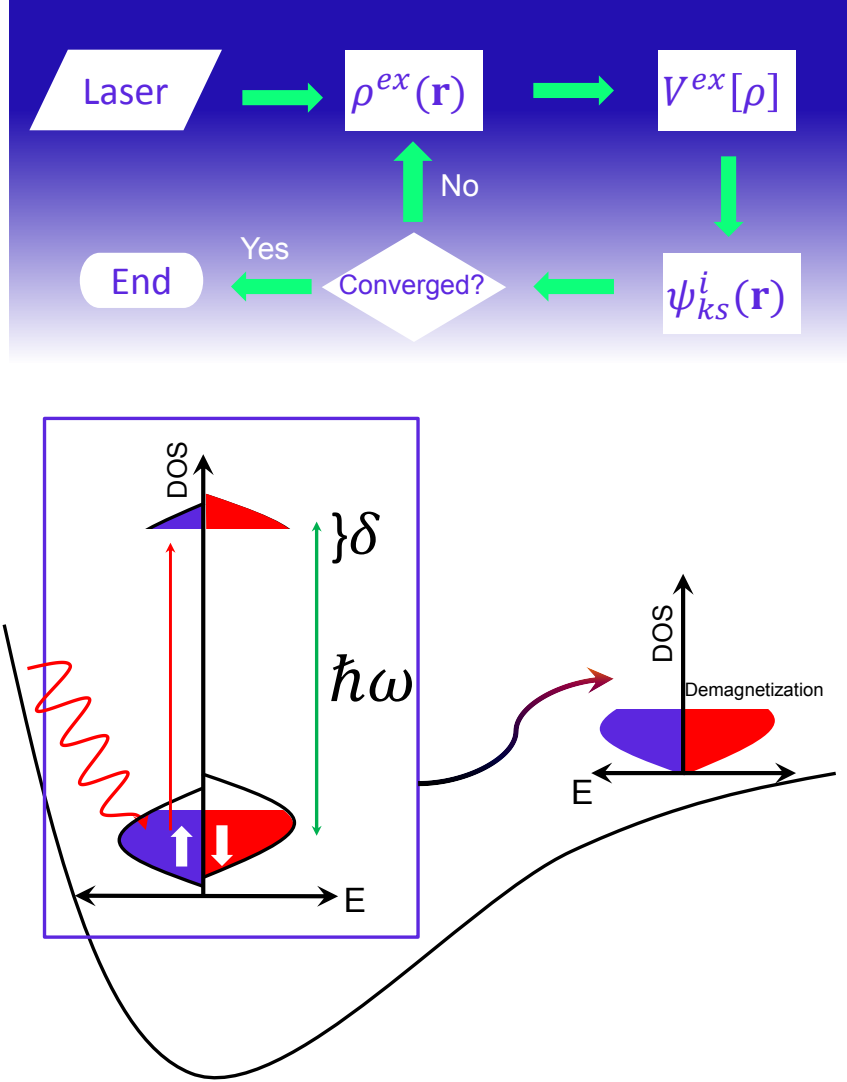


FIG. 1. Strong demagnetization induced on an excited potential surface. (Top) Computational scheme. The laser creates an excited charge density and excited potential energy surface for the entire system. By solving the Kohn-Sham (KS) equation, we attain the KS wavefunction for the next iteration until convergence. (Bottom) The laser excites only a very small number of electrons out of the Fermi sea, but the generated potential affects all the electrons. This drives the band structure relaxation, reduces the exchange splitting, and demagnetizes the sample. The laser excitation is determined by the photoenergy $\hbar\omega$, the width of the excitation δ (changing from 0.0 to 0.8 eV) and the strength of the excitation α (from 0.0 to 0.8, no unit).

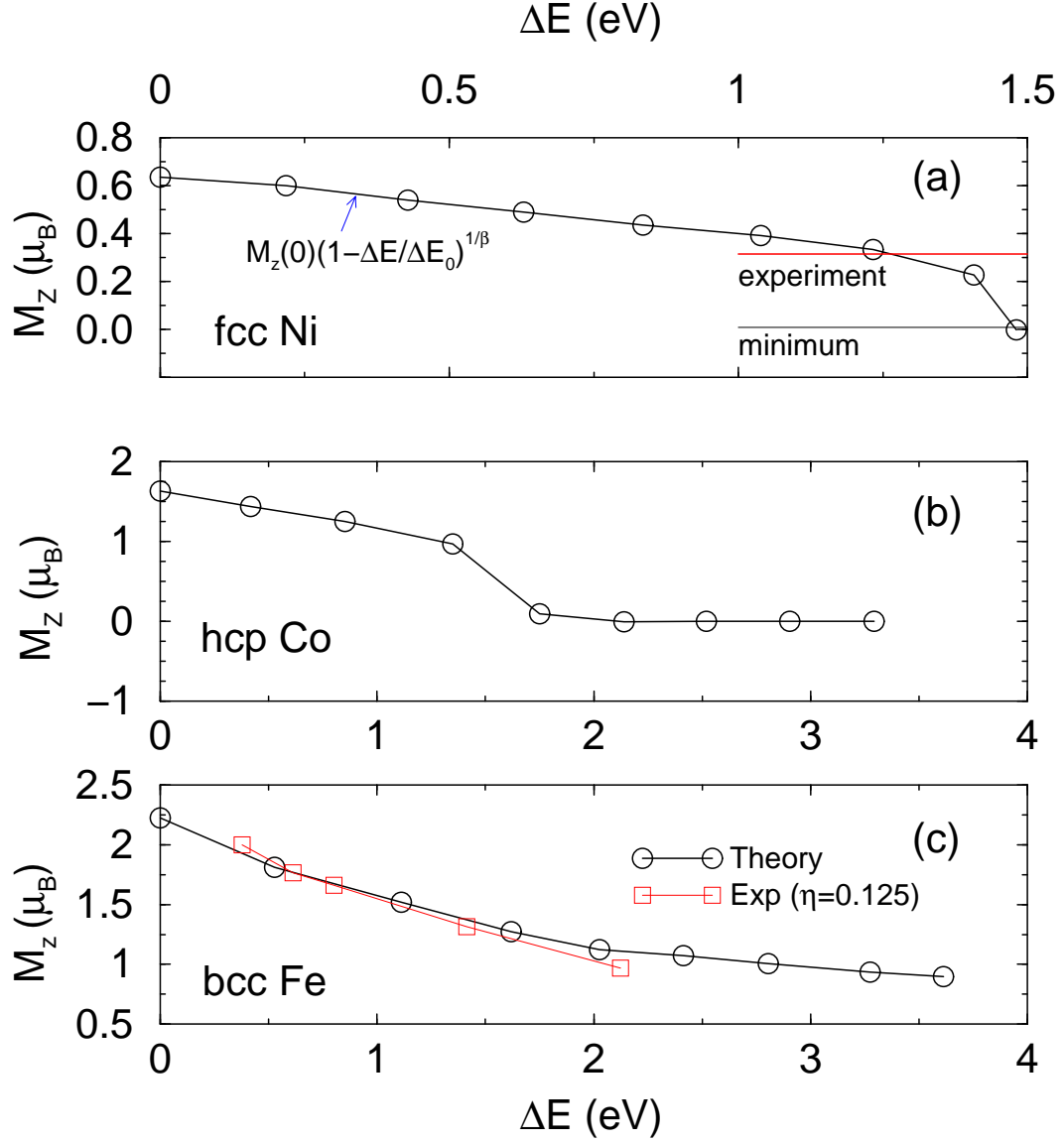


FIG. 2. Spin moment decreases as the energy absorbed increases for (a) fcc Ni, (b) hcp Co, and (c) bcc Fe. Here the photon energy is $\hbar\omega = 2.0$ eV, and the excitation window is fixed at $\delta = 0.5$ eV. For the same amount of energy absorbed by the system, fcc Ni is the easiest to be demagnetized, followed by hcp Co and bcc Fe, as expected from the strength of the magnetic ordering. In (a), a scaling function is shown. The experimental spin reduction is highlighted by a red line. In (c), the empty boxes represent the experimental results from Weber *et al.* [43], where the absorption efficiency factor η is 0.125.

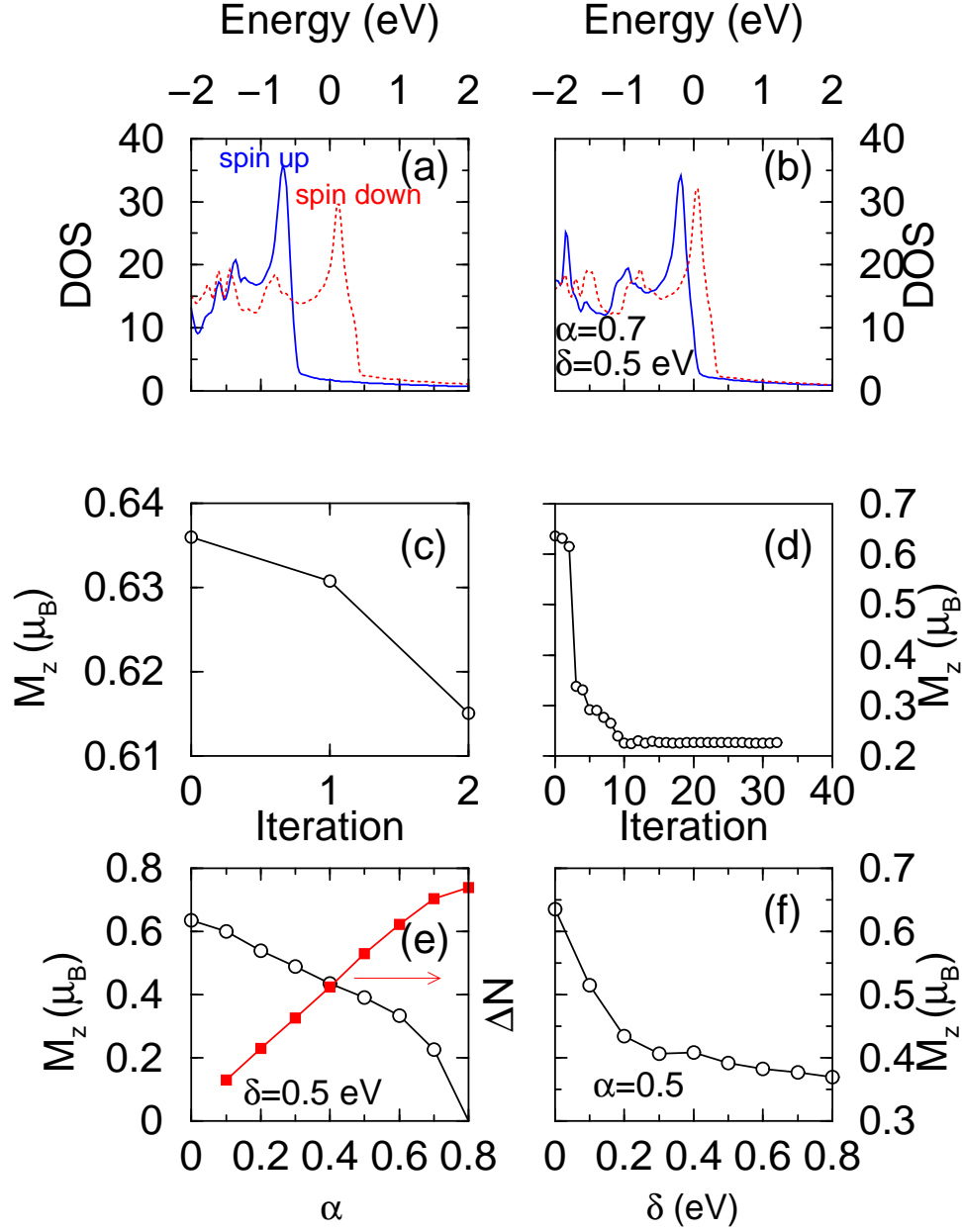


FIG. 3. (a) Density of d -states in pristine fcc Ni. The Fermi level is at 0 eV. (b) Density of d -states in the excited state, with the exchange splitting clearly reduced. Here the strength of excitation is $\alpha = 0.7$, the laser photon energy is $\hbar\omega = 2.0$ eV, and the width of the excitation is $\delta = 0.5$ eV. (c) Small spin moment change for the first two iterations. (d) Spin moment is sharply reduced as the self-consistent calculation iterates. Iteration 0 refers to the converged case without excitation. (e) Spin moment dependence (empty circles) on the excitation weight α for a fixed energy window ($\delta = 0.5$ eV). The filled boxes represent the number of electrons excited (Right axis). (f) Spin moment reduction as a function of the excitation window δ for a fixed excitation weight at $\alpha = 0.5$.